

Supporting Information

Quantitative Comparison of Dye and Ultrasmall Fluorescent Silica Core-Shell Nanoparticle Probes for Optical Super-Resolution Imaging of Model Block Copolymer Thin Film Surfaces

Joshua A. Hinckley,^{†,‡,§} Dana V. Chapman,^{†,§} Konrad R. Hedderick,[†] Katharine W. Oleske,[†] Lara A. Estroff,^{†,¶} and Ulrich B. Wiesner^{*,†}

[†]Department of Material Science and Engineering, Cornell University, Ithaca, New York 14853, United States

[‡]Department of Chemistry and Chemical Biology, Cornell University, Ithaca, New York 14853, United States

[§]Kavli Institute at Cornell for Nanoscale, Cornell University Science, Ithaca, New York 14853, United States

^{*}Corresponding Author Email: ubw1@cornell.edu

Materials.....	S2
Methods.....	S2
Polymer Synthesis.....	S2
Nanoparticle Synthesis	S3
Base srC' dot particle synthesis.....	S3
srC' dot purification	S4
srC' dot functionalization.....	S4
Nanoparticle Characterization.....	S5
Polymer Surface Functionalization	S7
AFM Imaging.....	S8
Super-Resolution Imaging	S9
TIRFM measurements	S9
Data analysis.....	S9
Data Selection	S11
Additional Data.....	S12
AFM BCP Swelling.....	S12
Localization SNR Comparison	S13
References	S14

Materials

Aluminum-tri-sec-butoxide (ASB), (3-aminopropyl) triethoxysilane (APTES), ammonium hydroxide (28 wt% in H₂O), ammonia solution (2.0 M in ethanol), dimethyl sulfoxide (DMSO), (3-mercaptopropyl) trimethoxysilane (MPTMS), 2-propanol (IPA, anhydrous 99.5%), tetramethyl orthosilicate (TMOS), Sulfo-Cy3(-)-DBCO, β -mercaptoethanol (β ME), glucose, and glucose oxidase were purchased from Sigma Aldrich. Catalase was purchased from Roche Applied Science. Methoxy-terminated poly(ethylene glycol) (PEG-silane, molar mass of ~0.5 kg/mol) was purchased from Gelest, Inc. Heterobifunctional PEGs with maleimide and N-Hydroxysuccinimide (NHS) ester groups (Mal-PEG₁₂-NHS; MW 865.92) and maleimide and DBCO groups (Mal-PEG₁₂-DBCO; MW 1027.161) were purchased from Quanta BioDesign. Thiol-PEG₃-azide was purchased from Conju-Probe, LLC. Negatively charged sulfo-Cy3(-)-NHS ester (free dye), positively charged Cy3(+)-NHS ester (encapsulated), negatively charged sulfo-Cy5(-)-NHS ester (free dye), and positively charged Cy5(+)-NHS ester (encapsulated) dyes were purchased from Lumiprobe Corp. All chemicals were used as received. Deionized (DI) water (18.2 M Ω ·cm) was generated using a Millipore Milli-Q system. P-type <100> silicon wafers were purchased from WRS Materials. Cysteamine, benzene, and methanol were purchased from Krackeler Scientific, Inc.

Methods

Polymer Synthesis

Two sizes of PS-*b*-P(AGE-*co*-EO) were synthesized by anionic polymerization as previous reported.^{1,2} Briefly, as follows: Benzene was cleaned and distilled into a dried reactor; styrene monomer was dried, degassed, and distilled into a burette. Sec-butyllithium was added to the reactor as the initiator followed by the distilled styrene, and the polymerization was carried out overnight. Hydroxy-terminated poly(styrene) (PS-OH) was synthesized by endcapping with ethylene oxide; the polymerization was terminated with degassed methanolic HCl. The reaction solution was washed and benzene removed from by distillation, and PS-OH was dried in the reactor on the Schlenk line at 130 °C for 3-4 days. PS-OH molar mass and dispersity were determined to be $M_n = 20,300$ g/mol and $\mathcal{D} = 1.02$ for the smaller block copolymer (BCP1) and $M_n = 58,000$ g/mol and $\mathcal{D} = 1.03$ for the larger block copolymer (BCP2) by

refractive index gel permeation chromatography (GPC) in unmodified tetrahydrofuran (THF) using PS standards. To polymerize the copolymer block, poly[(allyl glycidyl ether)-*co*-(ethylene oxide)] (P(AGE-*co*-EO)), cleaned THF was distilled into a separate burette and poured into the PS-OH reactor under nitrogen. (Note: Benzene and THF were cleaned over *n*-butyllithium. *Additional caution must be observed in working with n-butyllithium, as it is pyrophoric and will react violently in the presence of water.*) After dissolving PS-OH in THF, ~100 mg of potassium chloride were added to the reactor. The chain-end oxyanion was generated by adding 1-M potassium naphthalenide in THF until the solution turned green with the color persisting. AGE was stirred over butylmagnesium chloride for 30 minutes, distilled into an ampule, and kept frozen until cleaned EO was distilled directly onto the frozen AGE. The EO and AGE monomers were added to the reactor by inverse injection and polymerized for 4 days. The polymerization was terminated with degassed methanolic HCl, after which the THF in the reactor was exchanged for chloroform, and the washed polymer solution was precipitated into cold methanol. The resulting copolymers had dispersities of $\bar{D} = 1.08$ (BCP1) and $\bar{D} = 1.08$ (BCP2), as measured by THF GPC relative to PS standards. Molar mass was determined to be $M_n = 28,500$ g/mol for BCP1 and $M_n = 75,600$ g/mol for BCP2, as calculated by ^1H NMR and PS-OH molar masses.

Nanoparticle Synthesis

Base srC' dot particle synthesis: srC' dots were synthesized according to a previously published procedure.³ Briefly: 48 μL of Cy3(+)-NHS Ester (5 mg/1 mL in DMSO), 52 μL DMSO, and 4.46 μL APTES (0.084 M in DMSO) or 28 μL of Cy5(+)-NHS Ester (5 mg/0.5 mL in DMSO), 75 μL DMSO, and 4.46 μL APTES (0.084 M in DMSO) were combined in an inert nitrogen atmosphere in the dark. The mixture was allowed to react for 12 hours. Under vigorous stirring, a 60% molar ratio of MPTMS and TMOS were added into 10 mL of 0.2-M HCl (pH ~ 1.5) in a 25-mL round-bottom flask, immediately followed by the entire prepared Cy3(+)-silane dye solution and then 200 μL ASB. The mixture was allowed to react for 15 min; the particle growth was quenched by rapidly adding 150 μL PEG-silane (~0.5 kg/mol). 5 minutes after PEG-silane addition, the pH was adjusted by rapidly adding 100 μL of a 14%

aqueous solution of ammonia, raising the pH to ~8. The particles were stirred for another 12 hours, after which the stirring was terminated and the samples heated to 80 °C for 12 hours.

srC' dot purification: To increase silica nanoparticle (SNP) purity, we performed gel permeation chromatography (GPC) using a BioLogic LP system alongside a 275-nm UV detector with Sephacryl S-200 HR from GE Healthcare (Fig. S1). Particle solutions were up-concentrated by centrifuge spin-filters (GE Healthcare Vivaspın with MWCO 30K), sent through the column with a 0.9-wt% NaCl solution, and collected by a BioFrac fraction collector. The corresponding GPC fractions were transferred back into DI water by washing the particles at least 4 times in a spin-filter.

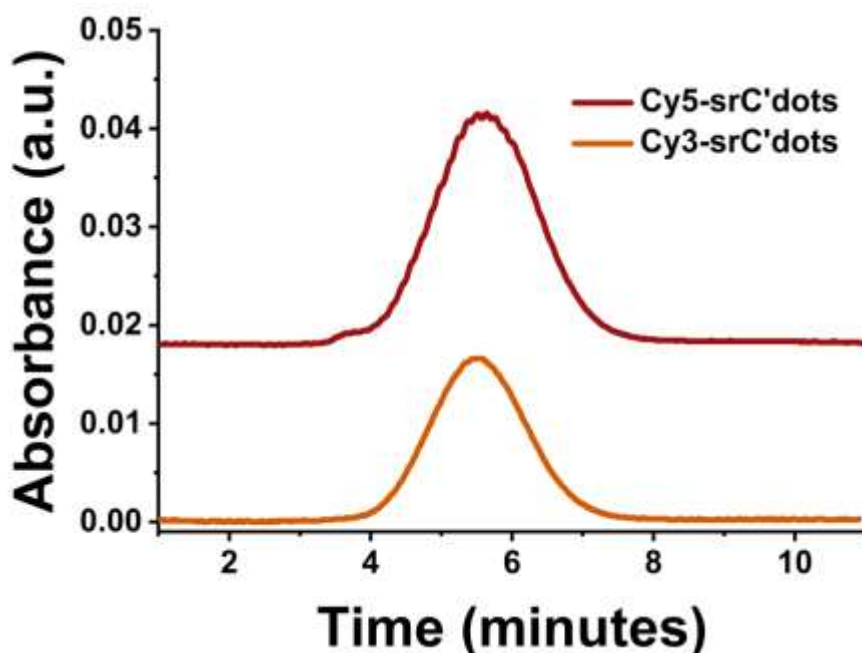


Figure S1. GPC chromatogram showing absorbance at 275 nm of Cy3(+)-srC'dots and Cy5(+)-srC'dots. The main peak at ~5.5 minutes corresponds to the desired srC'dot product.

srC' dot functionalization: Base SNPs were diluted to 1 μ M in water in a 4-mL vial under rapid stirring. Surface thiols formed during the nanoparticle synthesis **on the srC' dots** were used to attach heterobifunctional PEGs using maleimide-thiol click chemistry, as described elsewhere.⁴ Heterobifunctional PEGs were added at a ratio of 50 PEGs to 1 particle and were reacted overnight to ensure maximum attachment of the PEGs to the particle. To functionalize the **srC' dots** to be conjugated to the polymer using Chem1- and Chem2-STAMP, a maleimide-PEG₁₂-NHS ester was injected into the

1- μ M particle solution. For the former, a 1:1 molar ratio of cysteamine to maleimide-PEG₁₂-NHS ester was added and allowed to react in darkness with stirring for two hours at RT. A maleimide-PEG₁₂-DBCO was used to functionalize the srC' dots to be conjugated to the polymer using Chem3-STAMP. Final SNP absorbance spectra and FCS were not performed.

Nanoparticle Characterization

Particles were characterized using fluorescence correlation spectroscopy (FCS) (Fig. S2).⁵ To that end, a 543-nm continuous wave HeNe laser was reflected by a dichroic mirror and focused onto the object plane of a water immersion microscope objective (Zeiss Plan-Neofluar 63x NA 1.2). The fluorescence was collected by the same objective and spatially filtered by a 50- μ m pinhole located at the image plane of an avalanche photodiode detector (SPCM-AQR-14, PerkinElmer). Time traces were correlated by a hardware correlator card (Flex03LQ, Correlator.com). Tetramethylrhodamine (TMR) was used as a dye standard for the green laser line and Alexa Fluor 647 was used for the red line for system alignment and focal volume size determination due to its known diffusion coefficient.

Correlation data were collected in three sets of five 30-second runs. Correlation curves were then fit to a correlation function accounting for photoinduced *cis-trans* isomerization, as shown in equation (1):

$$G(\tau) = 1 + \frac{1}{N} \cdot \left(1 + \frac{\tau}{\tau_D}\right)^{-1} \cdot \left(1 + \frac{\tau}{\kappa^2 \tau_D}\right)^{-\frac{1}{2}} \cdot \frac{1}{1-T} \cdot \left(1 - T + T \cdot e^{-\frac{\tau}{\tau_F}}\right) \quad (1)$$

Here, N is the mean number of particles within the detection volume, κ is the structure factor determined by the ratio of the axial and radial radii (ω_z and ω_{xy} , respectively) of the observation volume, and τ_D is the characteristic diffusion time of an object through the observation volume. τ_D is defined as $\tau_D = \omega_{xy}/4D$, where D is the respective diffusion coefficient. T is the time- and space-averaged fraction of fluorophores in the *cis* photoisomer form, and τ_F is the characteristic relaxation time of the

photoisomerization process. The Stokes-Einstein relation, equation (2), was applied to determine particle diameters:

$$d = 2 \frac{k_b T}{6\pi\eta D} \quad (2)$$

Here, k_b is the Boltzmann constant, T is the temperature, and η is the dynamic viscosity. The average number of dyes per particle, n , was calculated according to equation (3):

$$n = \frac{C_{dye}}{C_{particle}} \quad (3)$$

Here, C_{dye} is the measured dye concentration derived from the dye extinction coefficient using the relative absorbance, and $C_{particle}$ is the particle concentration determined by FCS.

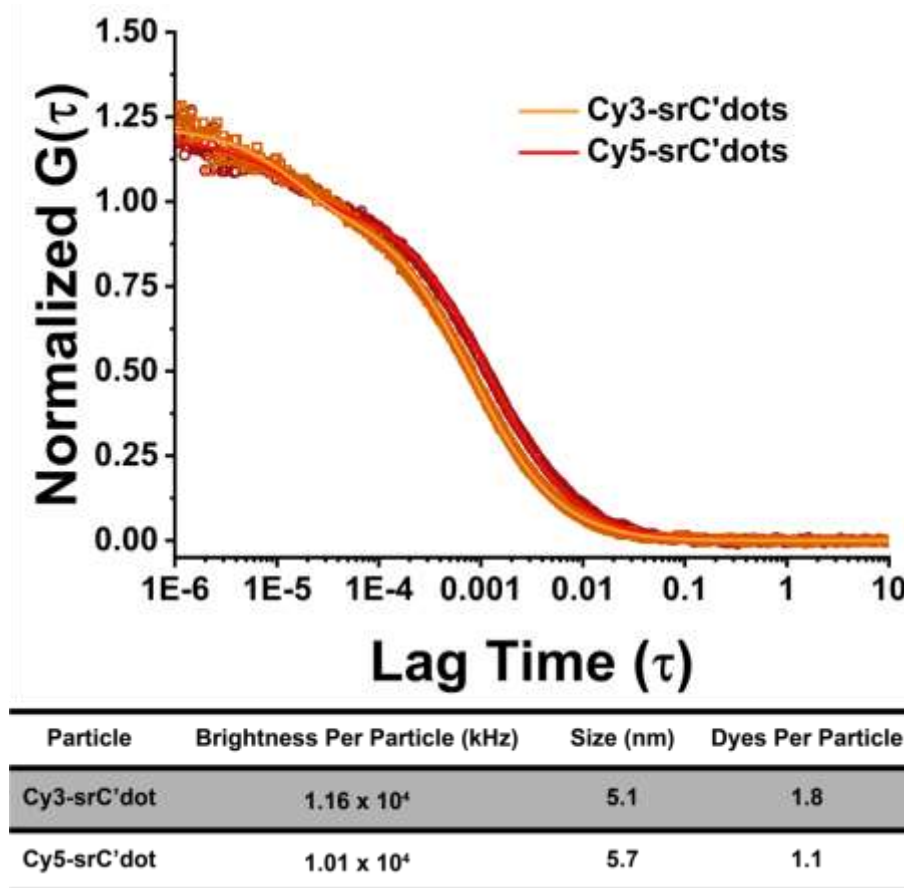


Figure S2. Fluorescence auto-correlation curve obtained for base particle srC' dots from FCS. Brightness per particle, size, and dyes per particle were obtained from the triplet-corrected FCS model in equation (1) and steady-state absorbance measurements shown in Fig. S3.

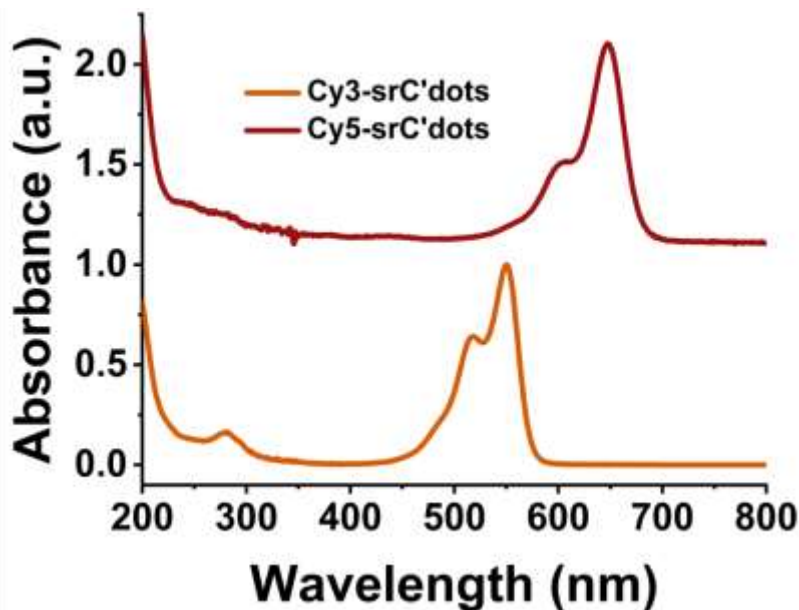


Figure S3. Steady-state absorbance spectra of the base particle srC' dots indicating an absorbance maxima around 550 nm for Cy3(+)-srC' dots and 647 nm for Cy5(+)-srC' dots.

Block Copolymer Thin Film Formation and Surface Functionalization

Single side-polished, P-type <100> silicon wafers were cut into ~1-cm² sized squares and sonicated in acetone for 15 minutes, sonicated in IPA for 15 minutes, rinsed with IPA, dried with N₂, and baked on a hot plate at 110 °C for 10 minutes. A 1.34-wt% solution of PS-*b*-P(AGE-*co*-EO) in benzene was spin-coated onto the cleaned silicon substrates and solvent vapor-annealed in a benzene-saturated atmosphere for 18 hours. The assembled thin films were dried and characterized using AFM.

In Chem1-STAMP (see Scheme 1), Cy3(+)-srC' dots end-functionalized with thiols were attached to the reactive film surface via thiol-ene click chemistry. The PS-*b*-P(AGE-*co*-EO) films were soaked in 10 mL 1:1 vol:vol mixture of water and methanol with 5 mM 2,2-dimethoxy-2-phenylacetophenone (DMPA), a photoinitiator, under 365-nm UV for 2 hours. Subsequently, the films

were washed four times with DI water to remove nanoparticles that were not selectively attached to the P(AGE-*co*-EO) block. In Chem2-STAMP, exposed AGE moieties were post-assembly functionalized with 1 M cysteamine under the same conditions as Chem1-STAMP, except that the UV exposure was extended to 8 hours. After washing the films four times in ethanol, srC' dots end-functionalized with NHS ester underwent reactions with the amine groups attached to the AGE moieties: The functionalized films were soaked in 10 mL 1:9 vol:vol dimethyl sulfoxide (DMSO)–water along with the NHS ester–functionalized Cy3(+)-srC' dots or with the Cy5(+)-srC' dots in darkness for 2 hours, after which the films were washed four times in DI water and dried. In Chem3-STAMP, films were soaked in 10 mL DMSO with [DMPA] = 5 mM and 0.09 mL of 10 wt% thiol-PEG₃-azide in DMSO under 365-nm UV for 8 hours; they were then washed four times with DI water. The azide end groups underwent further reaction in 10 mL water with DBCO-functionalized Cy3(+)-srC' dots in darkness for 1 hour, after which the films were washed four times in DI water and dried. For all sets of chemistries, reaction solutions were sparged using N₂ over a stir plate for 15 minutes, and the Cy3(+)-srC' dot concentration in the nanoparticle attachment step was 10 nM. Reaction solutions were agitated with stirring to prevent aggregation of nanoparticles. All conditions were maintained exactly the same for comparative analysis with attachment of the free dye (hydrophilic Cy3 derivative, sulfo-Cy3(-)-NHS ester, and sulfo-Cy5(-)-NHS ester) at 10 nM for Cy3 (both dye and srC' dots) on BCP1 and 100 nM for Cy5 (both dye and srC' dots) on BCP2 (to account for larger domain spacing and reduced accessibility to free allyl groups), except that the DBCO-sulfo-Cy3(-) was dissolved in 1 mL DMSO + 9 mL DI water.

AFM Imaging

All air AFM measurements of the block copolymer thin films were obtained using Tapping Mode on a Bruker MultiMode 8 in Atomic Force Microscope mode with Antimony (Sb)-doped silicon tips (Bruker RTESPA-150). Scans were obtained at a scan rate of 1-2 Hz. For fluid cell AFM measurements, the block copolymer thin films were presoaked in deionized water for 15 minutes before transferal to the AFM stage. All fluid cell AFM measurements were taken on the same instrument using a Bruker MTFML fluid cell holder and silicon nitride tips (Bruker DNP-S10) in Tapping Mode while deionized water (18.2 MΩ-cm, pH 5.8) was flowed over the sample at a rate of 0.3 mL/min. The sample was allowed to

equilibrate for 15 minutes in the fluid cell setup before images were captured. Scans were obtained at a scan rate of 1.5-2 Hz.

Super-Resolution Imaging

Total internal reflection fluorescence microscopy (TIRFM) measurements: Single-particle and single-molecule measurements were performed using an inverted Zeiss ELYRA microscope operated in TIRF geometry. Functionalized thin films on cleaned silicon substrates were inverted on a 1.5 cover glass mounted in an Attotfluor cell chamber (ThermoFisher Scientific) containing 1 mL of DI water combined with 5% (w/v) glucose, 50 μ L glucose oxidase (10 mg/mL in PBS), and 20 μ L catalase (2 mg/mL in PBS) as an enzymatic oxygen scavenging system. Samples were placed on an oil-immersion 1.46 NA 100X objective and simultaneously excited by a 561-nm laser and a 405-nm laser. Fluorescence signal was spectrally filtered using a 561-nm band-pass filter and recorded with an Andor iXon EMCCD camera. For each sample, multiple movies with a series of 10,000 frames and a resolution of 50 ms/frame were acquired. While the Cy3(+)-srC' dots do not need thiol-containing buffers for imaging,³ the sulfo-Cy3(-) required not only the oxygen scavenging system but also β -mercaptoethanol. An illustration of the imaging setup is shown in Fig. S4.

Data analysis: Photo-switching behavior of hundreds of different nanoparticles were studied using a custom-built MATLAB script described in reference 3. Localizations were fit to a Gaussian point spread function (PSF) as shown in equation (4):

$$PSF(x, y) = \frac{N}{2\pi\sigma^2} \cdot \exp\left(-\frac{(x-x_c)^2 + (y-y_c)^2}{2\sigma^2}\right) + b \quad (4)$$

where σ is the full-width at half-maximum (FWHM) of the localization and is equal to the localization uncertainty, N is the number of photons emitted by the probe, x_c and y_c are the sub-pixel coordinates, and b is the background. Reconstructed super-resolution STORM images were generated using ImageJ plugin ThunderSTORM.⁶

For Fig. 1a-d, the numbers of integrated photons of individual blinking events of free and encapsulated dyes, respectively, immobilized to block copolymer (BCP) surfaces were derived from the

respective TIRFM movies by fitting the spots to the Gaussian PSF, integrating the PSF, converting intensity to photons using the provided camera manufacturers photon conversion, and then plotting the results in the form of histograms.

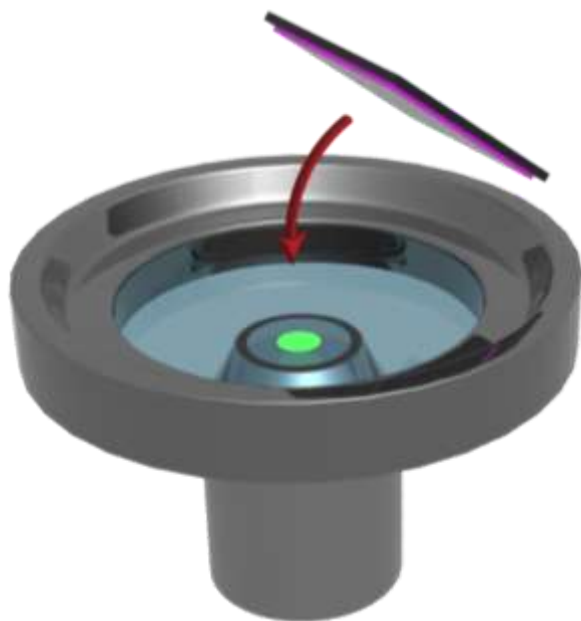


Figure S4. Illustration of the TIRFM setup, indicating thin film-bearing substrate (top), substrate loading position in Attofluor imaging well with 1.5 cover slip (middle), and microscope objective (bottom).

Data Selection

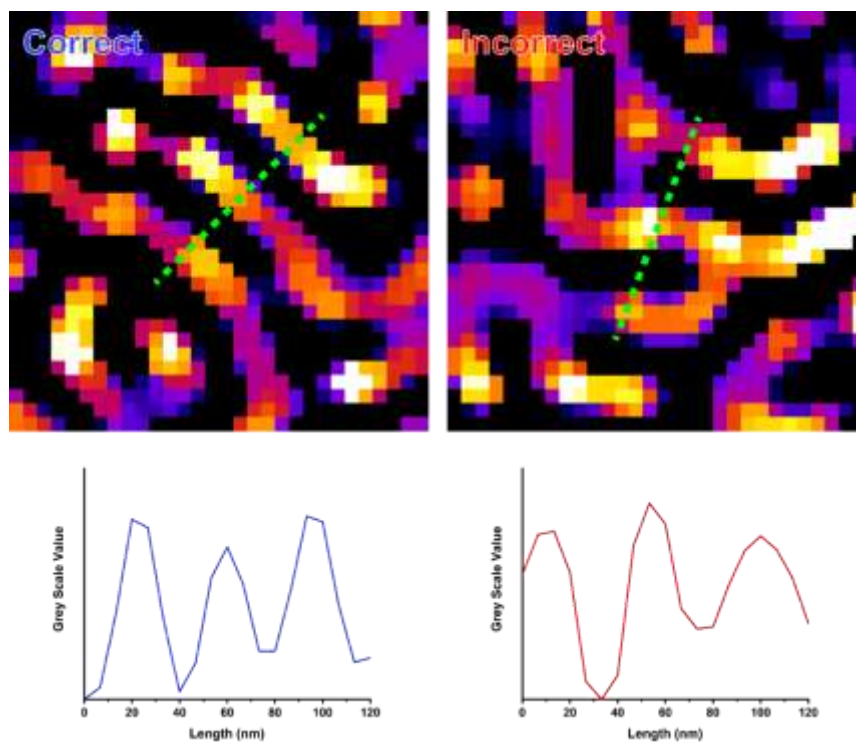


Figure S5. Super-resolution image-derived domain spacing from two different 200 nm by 200 nm BCP1 film areas. Domain spacings were measured for parallel domains as illustrated on the left side. The right side provides an example for an area with high-curvature BCP nanostructures, which usually leads to overestimations of BCP domain size. Line traces for both images (green lines) are shown at the bottom, illustrating the increased dimension for the curved sample. For consistency, AFM images were subjected to the same data analysis protocol.

Additional Data

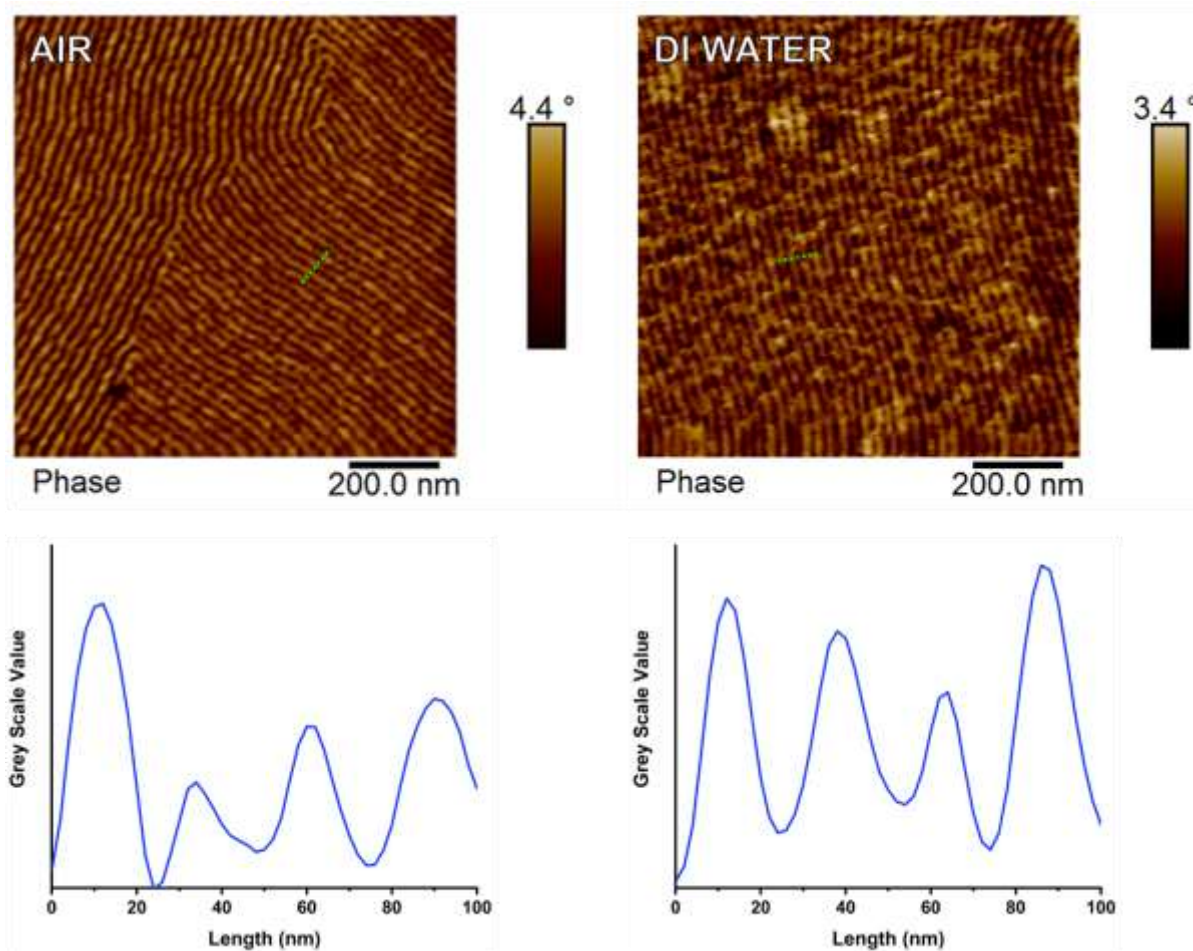


Figure S6. Fluid cell AFM phase images of the PS-*b*-P(AGE-*co*-EO) BCP1 film before and after swelling in water for roughly thirty minutes. Line profile analysis indicated that the domain spacing increased from $26.8 \text{ nm} \pm 4.5 \text{ nm}$ to $28.5 \text{ nm} \pm 5.1 \text{ nm}$ in DI water.

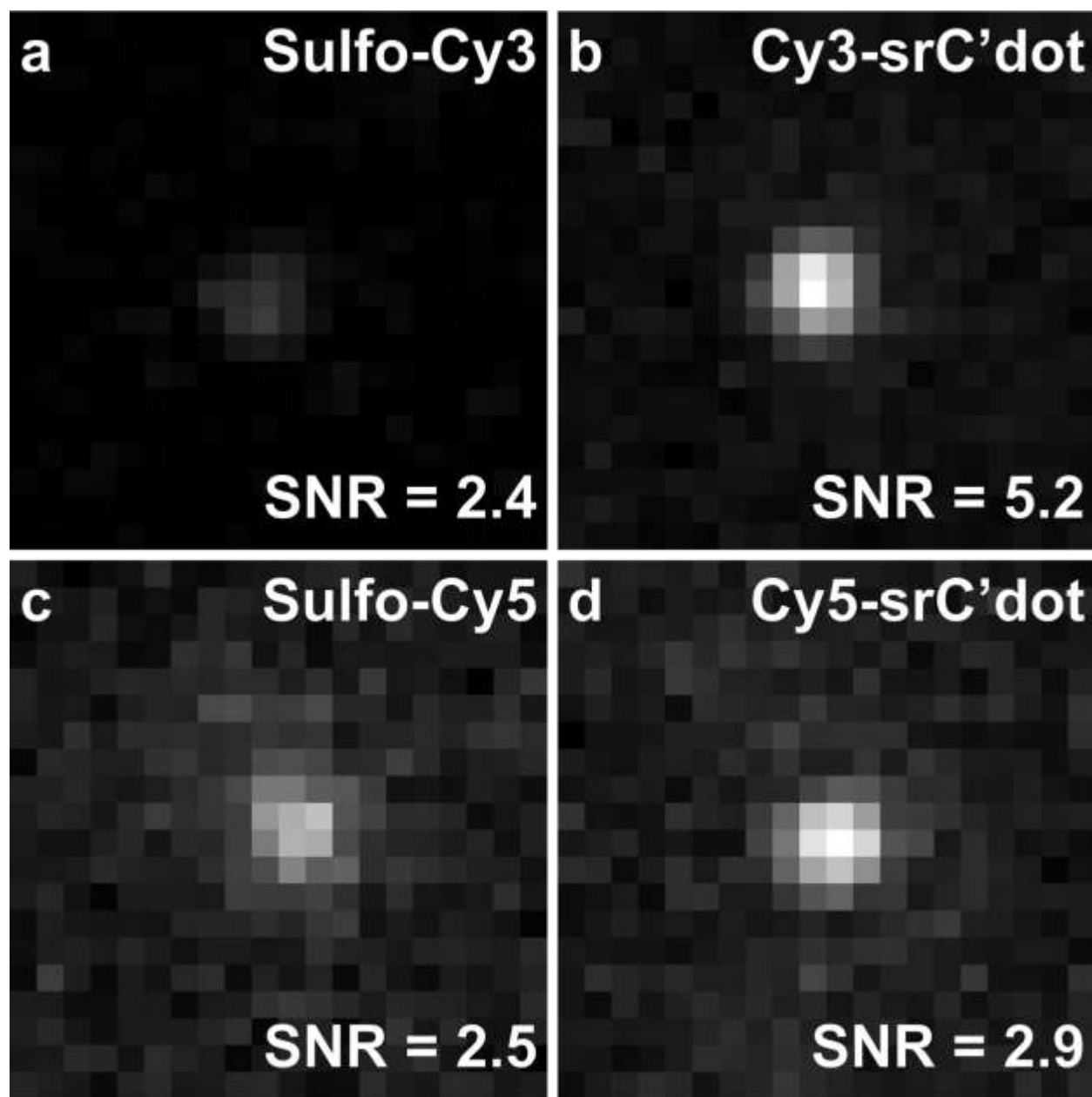


Figure S7. Example localization signal-to-noise comparisons for the four fluorescent probes. Contrast for the dye localization images were normalized to the contrast gray values of the corresponding srC' dot images.

References

- (1) Oleske, K. W.; Barteau, K. P.; Turker, M. Z.; Beaucage, P. A.; Estroff, L. A.; Wiesner, U. Block Copolymer Directed Nanostructured Surfaces as Templates for Confined Surface Reactions. *Macromolecules*. **2017**, *50* (2), 542–549.
- (2) Oleske, K. W.; Barteau, K. P.; Beaucage, P. A.; Asenath-Smith, E.; Wiesner, U.; Estroff, L. A. Nanopatterning of Crystalline Transition Metal Oxides by Surface Templated Nucleation on Block Copolymer Mesostructures. *Cryst. Growth Des.* **2017**, *17* (11), 5775–5782.
- (3) Kohle, F. F. E.; Hinckley, J. A.; Li, S.; Dhawan, N.; Katt, W. P.; Erstling, J. A.; Werner-Zwanziger, U.; Zwanziger, J.; Cerione, R. A.; Wiesner, U. B. Amorphous Quantum Nanomaterials. *Adv. Mater.* **2018**, *31* (5), 1806993.
- (4) Ma, K.; Wiesner, U. Modular and Orthogonal Post-PEGylation Surface Modifications by Insertion Enabling Penta-Functional Ultrasmall Organic-Silica Hybrid Nanoparticles. *Chem. Mater.* **2017**, *29* (16), 6840–6855.
- (5) Magde, D.; Elson, E.; Webb, W. W. Thermodynamic Fluctuations in a Reacting System Measurement by Fluorescence Correlation Spectroscopy. *Phys. Rev. Lett.*, **1972**, *29*, 705-708.
- (6) Ovesný, M.; Křížek, P.; Borkovec, J.; Švindrych, Z.; Hagen, G. M. ThunderSTORM: A Comprehensive ImageJ Plug-in for PALM and STORM Data Analysis and Super-Resolution Imaging. *Bioinformatics*. **2014**, *30* (16), 2389–2390.